

Cooling and heating by adiabatic magnetization in the $\text{Ni}_{50}\text{Mn}_{34}\text{In}_{16}$ magnetic shape-memory alloy

Xavier Moya, Lluís Mañosa,* and Antoni Planes

Departament d'Estructura i Constituents de la Matèria, Facultat de Física, Universitat de Barcelona, Diagonal 647, E-08028 Barcelona, Catalonia

Seda Aksoy, Mehmet Acet, Eberhardt F. Wassermann, and Thorsten Krenke[†]

Fachbereich Physik, Experimentalphysik, Universität Duisburg-Essen, D-47048 Duisburg, Germany

(Received 17 January 2007; published 14 May 2007)

We report on measurements of the adiabatic temperature change in the inverse magnetocaloric $\text{Ni}_{50}\text{Mn}_{34}\text{In}_{16}$ alloy. It is shown that this alloy heats up with the application of a magnetic field around the Curie point due to the conventional magnetocaloric effect. In contrast, the inverse magnetocaloric effect associated with the martensitic transition results in the unusual decrease of temperature by adiabatic magnetization. We also provide magnetization and specific heat data which enable to compare the measured temperature changes to the values indirectly computed from thermodynamic relationships. Good agreement is obtained for the conventional effect at the second-order paramagnetic-ferromagnetic phase transition. However, at the first-order structural transition the measured values at high fields are lower than the computed ones. Irreversible thermodynamics arguments are given to show that such a discrepancy is due to the irreversibility of the first-order martensitic transition.

DOI: [10.1103/PhysRevB.75.184412](https://doi.org/10.1103/PhysRevB.75.184412)

PACS number(s): 75.30.Sg, 64.70.Kb, 81.30.Kf

I. INTRODUCTION

When the magnetization of any magnetic material is changed isothermally under the application of a magnetic field, heat is exchanged with the surroundings. If the change is performed adiabatically, the temperature changes. This is the magnetocaloric effect (MCE), which provides the basis of the adiabatic demagnetization cooling technique.¹ This technique was developed to reach mK temperatures soon after the pioneering work by Debye² and Giauque,³ who independently suggested such a possibility. The discovery in the 1990s of the giant magnetocaloric effect associated with first-order magnetostructural transitions in a number of intermetallic alloy families⁴ opened up the possibility of using this technique in room temperature refrigeration applications and, thus, yielded renewed interest in the subject.⁵

It has been known for a long time that the isothermal reduction of a magnetic field gives rise to a decrease in entropy in some antiferromagnetic and ferrimagnetic systems.^{6,7} This inverse magnetocaloric phenomenon was supposed to produce small effects and has been largely ignored. Recently, however, it has been shown that in some ferromagnetic⁸ and metamagnetic⁹ systems, inverse MCE can have an amplitude comparable to the conventional effect detected in giant magnetocaloric intermetallic materials. The inverse effect is related to the existence of regions in phase space where $\zeta = (\partial M / \partial T)_H$ is positive. In a paramagnetic system, ζ is always negative, and thus, the origin of a positive ζ must be ascribed to coupling between magnetic moments. The inverse MCE can occur in the vicinity of magnetostructural and metamagnetic phase transitions due to changes in the magnetic coupling driven by the interplay between magnetic and structural degrees of freedom.¹⁰

In the present paper, we study the MCE in a $\text{Ni}_{50}\text{Mn}_{34}\text{In}_{16}$ alloy. This is a magnetic shape-memory alloy which under-

goes a martensitic transition from a cubic ($L2_1$) to a monoclinic ($10M$) structure below its Curie temperature.¹¹ Interestingly, the sample shows both inverse and conventional MCE in rather close temperature intervals. While the conventional effect arises from the continuous transition from paramagnetic to ferromagnetic states, the inverse effect is associated with the martensitic transition at which the magnetic moment of the system decreases. This decrease originates from the tendency of the excess of Mn atoms (with respect to 2-1-1 stoichiometry) to introduce antiferromagnetic coupling. The antiferromagnetic coupling is caused by the change in the Mn-Mn distance as the martensitic phase of lower symmetry gains stability.¹²

While most of the reported data on giant MCE materials refer to the isothermal entropy change, the most relevant parameter for actual applications of this effect is the adiabatic temperature change.¹³ This value is usually computed from entropy data by means of equilibrium thermodynamic relationships. However, irreversible effects are expected to take place at first-order phase transitions which can yield discrepancies between the computed temperature change and the directly measured one. Actually, direct measurements of the temperature change in giant MCE compounds are scarce, and the reported values in many cases do not seem to be consistent with those indirectly computed.¹⁴⁻¹⁶ Here, we report on adiabatic temperature measurements, which provide direct evidence of cooling by adiabatic magnetization in an inverse magnetocaloric material. It is also shown that heating is achieved at the paramagnetic-ferromagnetic phase transition. We focus on moderate magnetic fields which are readily available for applications of giant MCE materials.¹³ Furthermore, data obtained from magnetization and heat capacity experiments have enabled us to compare the measured temperature change with that computed from entropy data. Irreversible thermodynamics arguments are provided to account

for the discrepancies observed at the first-order structural phase transition.

II. EXPERIMENTAL DETAILS

A polycrystalline $\text{Ni}_{50}\text{Mn}_{34}\text{In}_{16}$ ingot was prepared by arc melting the pure metals under argon atmosphere in a water-cooled Cu crucible and subsequently remelted in order to ensure homogeneity. The ingot was sealed under argon in a quartz recipient and annealed at 1073 K for 2 hours. Finally, it was quenched in ice water. The composition of the alloy was determined by energy dispersive x-ray photoluminescence analysis. For calorimetric and magnetization measurements, a small sample (61.5 mg) was cut using a low-speed diamond saw. The remaining button (13 mm in diameter, 6 mm thickness, and 4.6 g) was used for the adiabatic temperature change measurements.

Magnetization was measured by means of a superconducting quantum interference device (SQUID) magnetometer, and differential scanning calorimetric (DSC) measurements were conducted using a high-sensitivity calorimeter. Specific heat measurements were performed using a modulated differential scanning calorimeter, and data were taken with the constant temperature method¹⁷ starting from the lowest temperature (190 K).

Adiabatic temperature changes were measured at atmospheric pressure using a specially designed setup. A thin (0.75 mm diameter) Ni-Cr/Ni-Al thermocouple was used to measure the temperature. The output of this thermocouple was continuously monitored by means of a multimeter that also electronically compensates for the reference junction. Measurements without any specimen confirmed that the recorded values were not affected by magnetic fields up to 1.3 T. The thermocouple was embedded within the sample and good thermal contact between the sample and the thermocouple was ensured by Ariston conductive paste. The sample is situated inside a copper container (sample holder), which is placed on the top face of a Peltier element. The bottom surface sits on a copper cylinder, which acts as a heat sink. The bottom end of the cylinder is in contact with a nitrogen bath. By controlling the current input into the Peltier element, it is possible to achieve fine tuning of the temperature in the 200–320 K interval. Temperature oscillations were less than 0.05 K. Thermal insulation (adiabaticity) between the sample and sample holder was ensured by a polystyrene layer. The sample holder was placed in between the poles of an electromagnet (28 mm gap), which enabled fields up to 1.3 T to be applied. A major advantage of using an electromagnet is the short rising time in the application of the field (the field rises from 0 to 1 T in about 0.5 s). Such a field risetime is several orders of magnitude shorter than the thermal relaxation time of the sample-holder system (~ 100 s), thus ensuring the adiabaticity of the process.

In order to check the reliability of the device, we measured the MCE of commercial pure (99.9 wt %) Gd. The measured temperature changes obtained around the Curie point for a magnetic field of 1 T agree with those reported in the literature.¹⁸

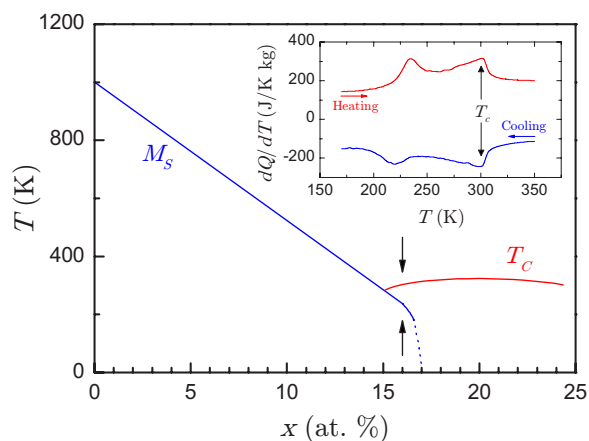


FIG. 1. (Color online) Phase diagram of $\text{Ni}_{50}\text{Mn}_{50-x}\text{In}_x$, obtained using the data in Ref. 11. M_s indicates the martensitic transition line and T_c indicates the Curie point line. The inset shows DSC curves for heating and cooling runs for the $x=16$ sample.

III. RESULTS AND DISCUSSION

For the present study we selected a composition with the para-ferromagnetic and martensitic transition temperatures close to each other. This is illustrated in Fig. 1, which shows the Curie and martensitic transition start temperatures as a function of In content for $\text{Ni}_{50}\text{Mn}_{50-x}\text{In}_x$ alloys. Continuous lines are polynomial fits to the data given in Ref. 11. The arrows indicate the composition of the studied sample. The inset presents DSC curves (heating and cooling) for the present $\text{Ni}_{50}\text{Mn}_{34}\text{In}_{16}$ alloy.¹⁹ The peaks at higher temperature correspond to the Curie point and those at lower temperatures correspond to the martensitic transition (which occurs with 15 K thermal hysteresis). Integration of the peaks associated with the martensitic transition renders latent heats of -1750 ± 100 J/kg for the cooling run (forward transition) and 1850 ± 100 J/kg for the heating run (reverse transition).

The adiabatic temperature changes measured over the 200–320 K temperature range for selected values of the magnetic field are shown in Fig. 2(a). Data points were obtained according to the following procedure, which ensures the suppression of any history dependent effect: first, the sample is heated up to 320 K (above the Curie point) and then cooled down to the fully martensitic state at 170 K. Subsequently, it is heated up to the desired temperature and the magnetic field is switched on for 20 s. After switching off the field, the sample is heated again above the Curie point and the protocol is repeated for the next data point. The measured adiabatic temperature changes shown in Fig. 2(a) prove unambiguously that the sample cools down upon adiabatic application of the field in the temperature range 200–245 K, while it heats up in the temperature range 245–320 K. The positive temperature change has its maximum value ($\Delta T \approx 1.5$ K for 1.3 T) at the Curie point. The maximum temperature decrease ($\Delta T \approx -0.6$ K for 1.3 T) occurs at a temperature that shifts with magnetic field [see inset in Fig. 2(a)], in agreement with the decrease in the martensitic transition temperature reported for Ni-Mn-In alloys.¹¹ The values found for ΔT at their corresponding peak temperatures are comparable to those reported for other giant

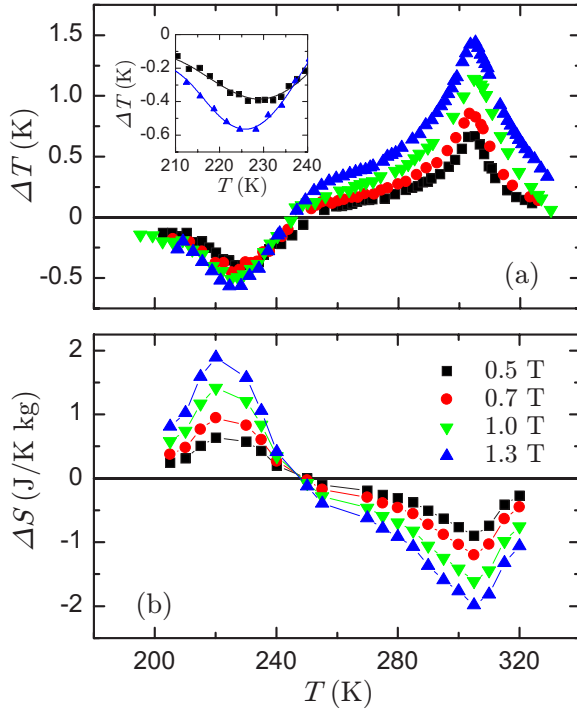


FIG. 2. (Color online) (a) Measured adiabatic temperature change and (b) computed isothermal entropy change, as a function of temperature at selected values of the magnetic field. The inset shows an enlarged view for the 0.5 and 1.3 T fields which illustrates the shift in the inverse MCE with magnetic field.

MCE materials. However, a feature for $\text{Ni}_{50}\text{Mn}_{34}\text{In}_{16}$ is that these relatively large temperature changes can be either positive or negative.

In order to correlate the measured temperature changes with those indirectly computed from entropy data, we measured the magnetization of the sample as a function of temperature and magnetic field. Results at selected fields are shown in Fig. 3(a). In the temperature range 245–320 K, ζ is negative, while a positive ζ is obtained in the range

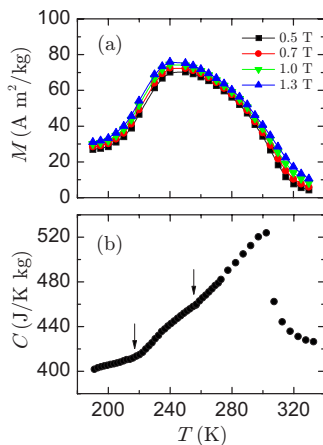


FIG. 3. (Color online) (a) Temperature dependence of the magnetization for selected values of the magnetic field. (b) Specific heat as a function of temperature. Arrows indicate the region of the reverse martensitic transition.

200–245 K. From these data, we computed the magnetic field-induced entropy change by using the Maxwell relation $\Delta S = \mu_0 \int \zeta dH$. Results are shown in Fig. 2(b). Excellent qualitative agreement is observed between the two quantities (ΔT and ΔS) characterizing giant MCE. Conventional MCE is observed within the 245–320 K temperature range, i.e., a negative entropy change with the associated positive temperature change, while in the 200–245 K interval, the sample exhibits inverse MCE: an increase in entropy with the associated negative temperature change.

It is customary to compute the adiabatic temperature change from isothermal entropy data by means of the following relationship:

$$\Delta T_{\text{rev}} = -\frac{T}{C}\Delta S, \quad (1)$$

which is expected to be valid in equilibrium. C is the specific heat at constant magnetic field and is assumed to be independent of the magnetic field. In order to check the validity of this approach, we measured the specific heat of our $\text{Ni}_{50}\text{Mn}_{34}\text{In}_{16}$ sample. Results are shown in Fig. 3(b). The large lambda-type peak at 302 K corresponds to the second-order para-ferromagnetic phase transition. In the temperature range 216–257 K a small bump is observed, which coincides with the reverse martensitic transition. No latent heat contributions are expected for the isothermal-modulated method we have used.

In Fig. 4, we compare the measured adiabatic temperature changes with those computed from the entropy [Fig. 2(b)] and specific heat data [Fig. 3(b)] for different values of the applied field. Good agreement between measured and computed values over the complete temperature range is obtained at low magnetic fields. As the magnetic field is increased, there is still good agreement between the data corresponding to conventional MCE,²⁰ but the absolute value of the measured temperature change becomes smaller than the computed one in the inverse MCE region. Such a difference is due to the irreversibility associated with the first-order phase transition.

In order to consider the effect of dissipation, we start from the Clausius inequality $\oint \frac{\delta q}{T} \leq 0$, which can be expressed as $\frac{\delta q}{T} = dS - \delta S_i$, where dS is a reversible differential change of entropy and δS_i is the entropy production ($\delta S_i \geq 0$). When the magnetic field is adiabatically changed, $\delta q = 0$, and under the assumption of a quasistatic, continuous process with hysteresis,²¹ the adiabatic temperature change is expressed as

$$\Delta T = \frac{T}{C}(-\Delta S + S_i) = \Delta T_{\text{rev}} + \frac{TS_i}{C}, \quad (2)$$

where TS_i is the dissipated energy (E_{diss}). For an inverse magnetocaloric effect, there is an increase of entropy by the application of the field, i.e., $\Delta S > 0$. On the other hand, S_i is always positive. Hence, for an out-of-equilibrium process, the two terms within the parentheses in Eq. (2) will partially cancel each other when the field is swept from zero to a given value, and therefore, the measured temperature change will always be less than the value computed using equilibrium thermodynamics [see Eq. (1)]. Such a difference is ex-

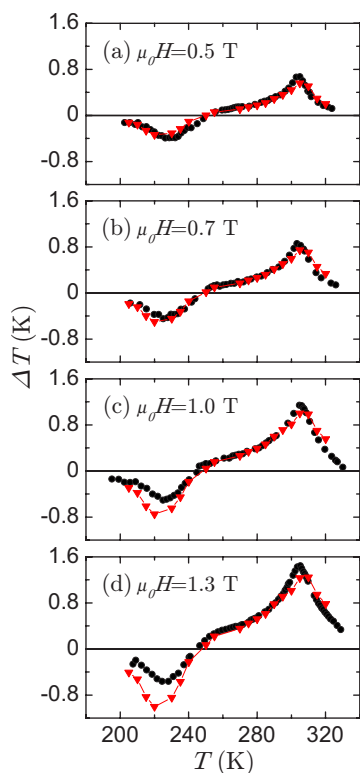


FIG. 4. (Color online) Adiabatic temperature change, as a function of temperature, for different magnetic fields. Circles stand for measured data and triangles correspond to data indirectly computed using equilibrium thermodynamics relationships.

pected to be small at low fields (close to equilibrium conditions), but it becomes larger at higher fields. Note that for conventional MCE, when the field changes from 0 to H , $\Delta T \geq \Delta T_{\text{rev}}$, which is consistent with the data around the Curie point.

At each temperature, the dissipated energy is given by $E_{\text{diss}} = T\Delta S + C\Delta T$. A value of 158 J/kg is found at 225 K for a field of 1.3 T. This value amounts to about 10% of the latent heat of the martensitic transition in this alloy.

In giant magnetocaloric materials for which the MCE is associated with a first-order transition, the giant effect relies on the possibility of inducing the phase transition by application of a magnetic field. The martensitic transition is driven by phonon instabilities in the transverse TA_2 phonon branch ($[110]$ propagation and $[1\bar{1}0]$ polarization).^{22,23} Recent *ab initio* calculations for cubic Ni_2MnIn have shown that increasing the magnetization due to an external field favors the cubic structure and leads to a gradual vanishing of the phonon instability²⁴ due to the coupling between vibrational and magnetic degrees of freedom. This effect results in a marked decrease of the martensitic transition temperature with increasing field that enables to induce the transition by the application of a field at a temperature close to the zero field transition temperature. Hence, the microscopic origin of the inverse MCE in $\text{Ni}_{50}\text{Mn}_{34}\text{In}_{16}$ must be ascribed to such magnetoelastic coupling responsible for the change in the relative stability of the martensitic and cubic phases.

IV. CONCLUSION

By directly measuring the adiabatic temperature change in the $\text{Ni}_{50}\text{Mn}_{34}\text{In}_{16}$ alloy, we provide experimental evidences of both cooling and heating in a giant inverse magnetocaloric compound. It has been shown that the irreversibility associated with the first-order structural transition gives rise to measured temperature changes which are lower than those indirectly computed using equilibrium thermodynamics. The existence of a temperature region where the magnetocaloric effect reverses sign under weakly applied magnetic fields opens up the possibility of new applications of this fascinating property.

ACKNOWLEDGMENTS

This work received financial support from the CICYT (Spain), Contract No. MAT2004-01291, DURSI (Catalonia), Contract No. 2005SGR00969, and from the Deutsche Forschungsgemeinschaft (Contract No. GK277). One of the authors (X.M.) acknowledges support from DGICYT (Spain). The authors thank Peter Hinkel for technical support.

*Electronic address: lluis@ecm.ub.es

†Present address: ThyssenKrupp Electrical Steel GmbH, D-45881 Gelsenkirchen, Germany.

¹A. M. Tishin and Y. I. Spinchkin, *The Magnetocaloric Effect and its Applications* (Institute of Physics, Bristol, 2003).

²P. Debye, *Ann. Phys.* **81**, 1154 (1926).

³W. F. Giauque, *J. Am. Chem. Soc.* **49**, 1864 (1927).

⁴V. K. Pecharsky and K. A. Gschneidner, *Phys. Rev. Lett.* **78**, 4494 (1997); for a thorough and comprehensive review of new magnetocaloric materials see, K. A. Gschneidner, V. K. Pecharsky, and A. O. Tsokol, *Rep. Prog. Phys.* **68**, 1479 (2005).

⁵E. Brück, *J. Phys. D* **38**, R381 (2005).

⁶R. J. Joenk, *Phys. Rev.* **128**, 1634 (1962).

⁷A. E. Clark and E. Callen, *Phys. Rev. Lett.* **23**, 307 (1969).

⁸T. Krenke, M. Acet, E. F. Wassermann, X. Moya, L. Mañosa, and A. Planes, *Nat. Mater.* **4**, 450 (2005).

⁹K. G. Sandeman, R. Daou, S. Özcan, J. H. Durrell, N. D. Mathur, and D. J. Fray, *Phys. Rev. B* **74**, 224436 (2006).

¹⁰A. Planes, L. Mañosa, and A. Saxena, in *Interplay of Magnetism and Structure in Functional Materials*, edited by A. Planes, L. Mañosa, and A. Saxena, Materials Science Series Vol. 79 (Springer-Verlag, Berlin, 2005).

¹¹T. Krenke, M. Acet, E. F. Wassermann, X. Moya, L. Mañosa, and A. Planes, *Phys. Rev. B* **73**, 174413 (2006); T. Krenke, E. Duman, M. Acet, E. F. Wassermann, X. Moya, L. Mañosa, A. Planes, E. Suard, and B. Ouladdiaff, *ibid.* **75**, 104414 (2007).

¹²P. J. Brown, A. P. Gandy, K. Ishida, R. Kainuma, T. Kanomata, K. U. Neumann, K. Oikawa, B. Ouladdiaff, and K. R. A. Ziebeck, *J.*

- Phys.: Condens. Matter **18**, 2249 (2006).
- ¹³V. K. Pecharsky and K. A. Gschneidner, Int. J. Refrig. **29**, 1239 (2006).
- ¹⁴A. Giguère, M. Foldeaki, B. Ravi Gopal, R. Chahine, T. K. Bose, A. Frydman, and J. A. Barclay, Phys. Rev. Lett. **83**, 2262 (1999).
- ¹⁵K. A. Gschneidner, V. K. Pecharsky, E. Brück, H. G. M. Duijn, and E. M. Levin, Phys. Rev. Lett. **85**, 4190 (2000).
- ¹⁶M. Pasquale, C. P. Sasso, L. H. Lewis, L. Giudici, T. Lograsso, and D. Schlagel, Phys. Rev. B **72**, 094435 (2005).
- ¹⁷A. Boller, Y. Jin, and B. Wunderlich, J. Therm. Anal. **42**, 307 (1994).
- ¹⁸S. Y. Dan'kov, A. M. Tishin, V. K. Pecharsky, and K. A. Gschneidner, Phys. Rev. B **57**, 3478 (1998).
- ¹⁹The shape of the thermograms shown in Fig. 1 differs from those reported in Ref. 11 because they correspond to different specimens. Unavoidable small composition inhomogeneities, impurities, etc., are known to affect the actual transition path. Therefore, different thermograms can be obtained in different specimens with the same nominal composition.
- ²⁰The small discrepancies in the data around the Curie point arise from the fact that the specific heat has been considered to be independent of the magnetic field. For ferromagnetic materials the effect of magnetic field is to smooth out the peak in the specific heat.
- ²¹J. Ortín, A. Planes, and L. Delaey in *The Science of Hysteresis*, edited by I. Mayergoyz and G. Bertotti, (Elsevier, New York, 2005), Vol. 3, p. 467.
- ²²A. Planes and L. Mañosa, Solid State Phys. **55**, 159 (2001).
- ²³P. Entel, V. D. Buchelnikov, V. V. Khovailo, A. T. Zayak, W. A. Adeagbo, M. E. Gruner, H. C. Herper, and E. F. Wassermann, J. Phys. D **39**, 865 (2006).
- ²⁴P. Entel, M. E. Gruner, W. A. Adeagbo, and A. T. Zayak, Mater. Sci. Eng., A (to be published).